Supplementary Information

Inverse design of metasurfaces with non-local interactions

Haogang Cai,[1,2*] Srilok Srinivasan,[1] David Czaplewski,[1] Alex Martinson,[3] David Gosztola,[1] Liliana Stan,[1] Troy Loeffler,[1] Subramanian K. R. S. Sankaranarayanan,[1,4*] Daniel López[1*]

[1] Center for Nanoscale Materials, Argonne National Laboratory, Lemont, IL, 60439, USA.
[2] Present address: Tech4Health Institute and Department of Radiology, NYU Langone Health, New York, NY, 10016 USA.
[3] Materials Science Division, Argonne National Laboratory, Lemont, IL, 60439, USA.
[4] Department of Mechanical and Industrial Engineering, University of Illinois, Chicago, IL 60607, USA

*email: haogang.cai@nyu.edu, skrssank@uic.edu, omardaniellopez@gmail.com

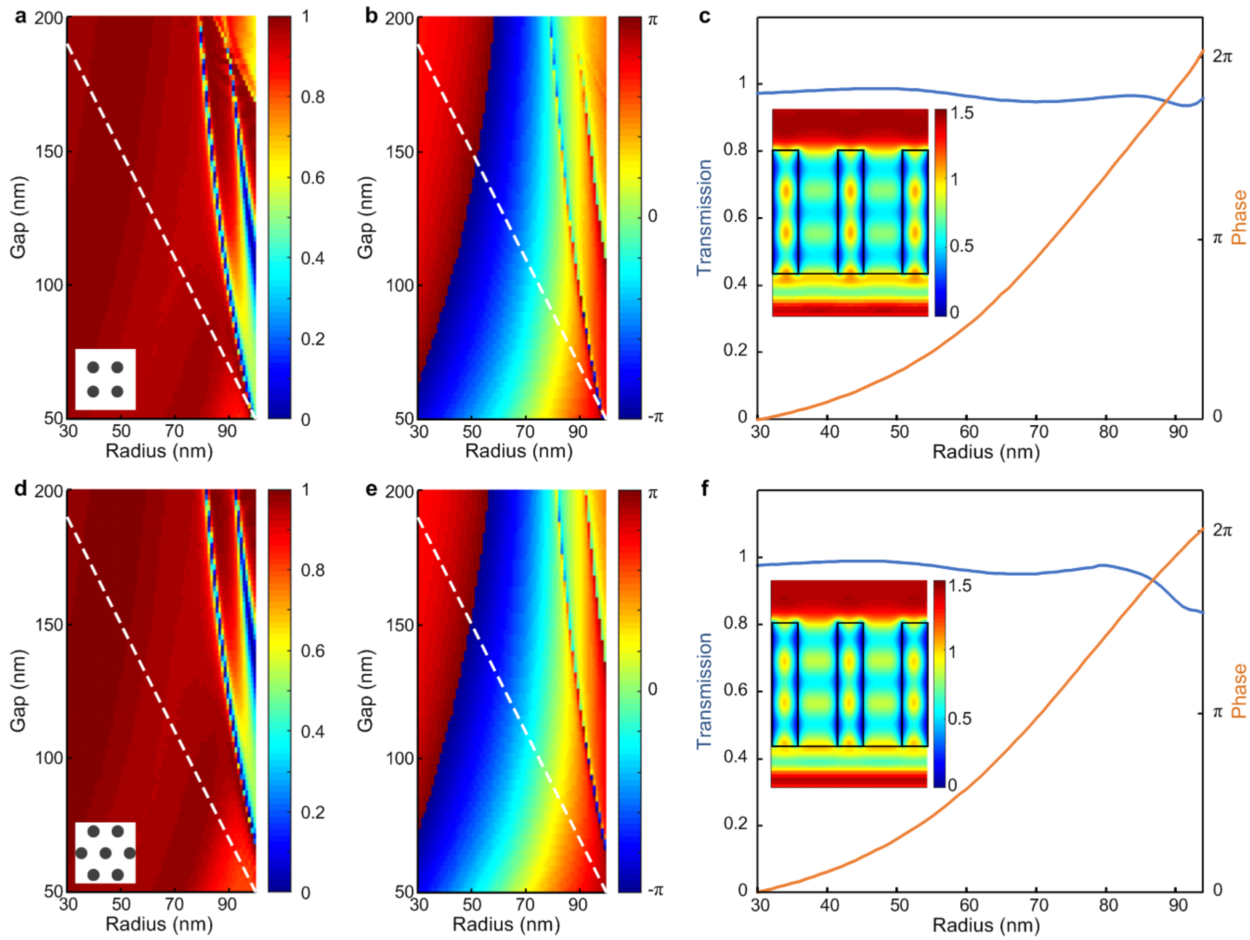

Supplementary Fig. 1 Effect of the interactions between high-aspect-ratio waveguide-type meta-atoms on the amplitude and phase of the transmitted light. FDTD simulation results of the transmission and phase shift experienced by a uniform wavefront of light after propagation through a homogeneous and periodic nanoresonator array (circular TiO_2 nanopillars, thickness t = 600 nm, on glass substrate). Square arrays: (a) transmission and (b) phase shift as a function of the pillar radius and edge-to-edge gap; (c) transmission and phase for a meta-atom library with constant pitch of 250 nm and varying pillar radius (following the path marked by white dashed lines in a, b). Hexagonal arrays: (d) transmission and (e) phase shift as a function of the pillar radius and edge-to-edge gap; (f) transmission and phase for the same library with constant pitch (250 nm) and varying pillar radius in hexagonal arrangement. The insets in c, f show the side views of the electric energy density in a meta-atom array (pitch 250 nm, radius 60 nm) for square and hexagonal arrangements, respectively.

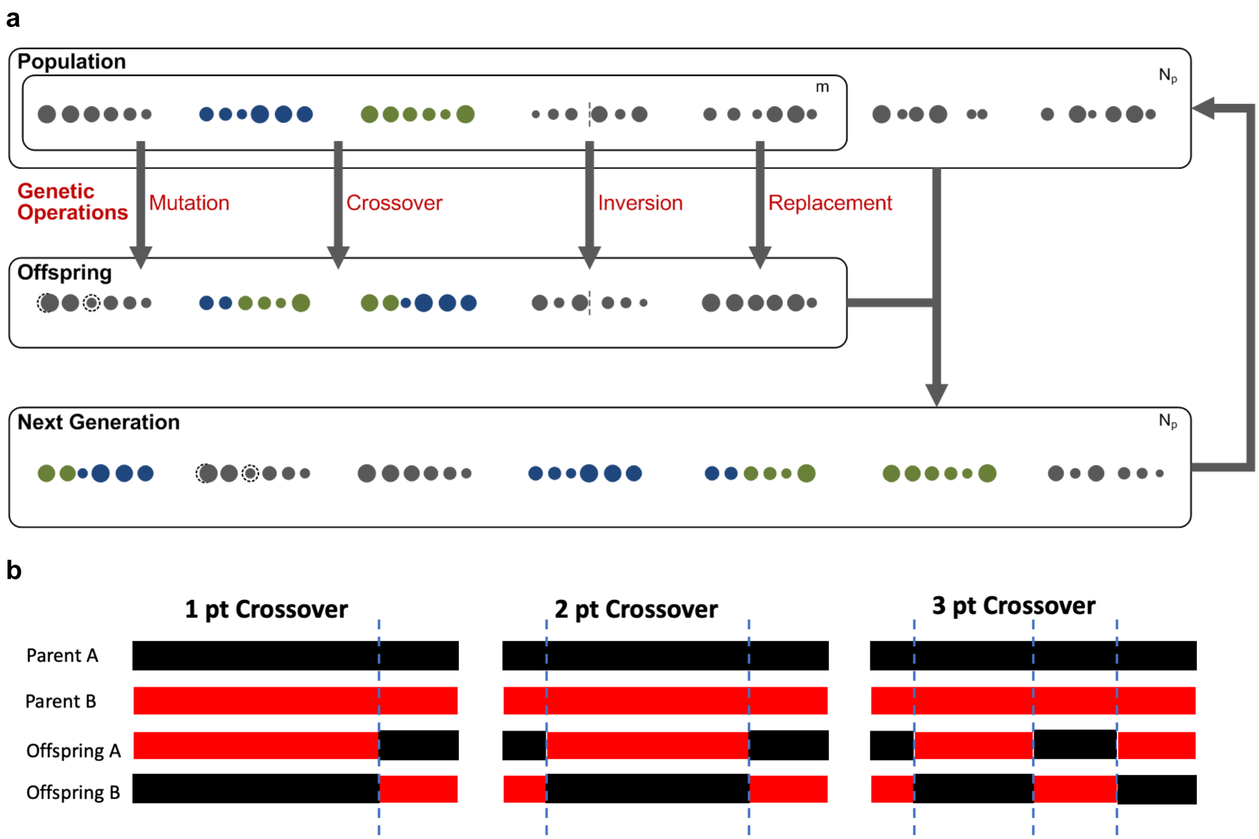

Supplementary Fig. 2 Details of the evolutionary optimization for inverse design. (a) Schematic diagram of the evolutionary optimization flow and genetic operations. (b) Crossover operations: the parent structures are sliced and the resulting slices are swapped to produce the offspring.

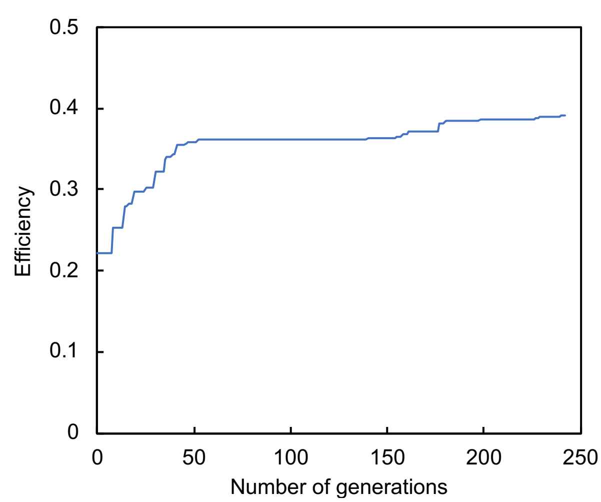

Supplementary Fig. 3 Evolutionary optimization convergence curve. Focusing efficiency vs. number of generations in the genetic algorithm for a cylindrical lens with NA = 0.77.

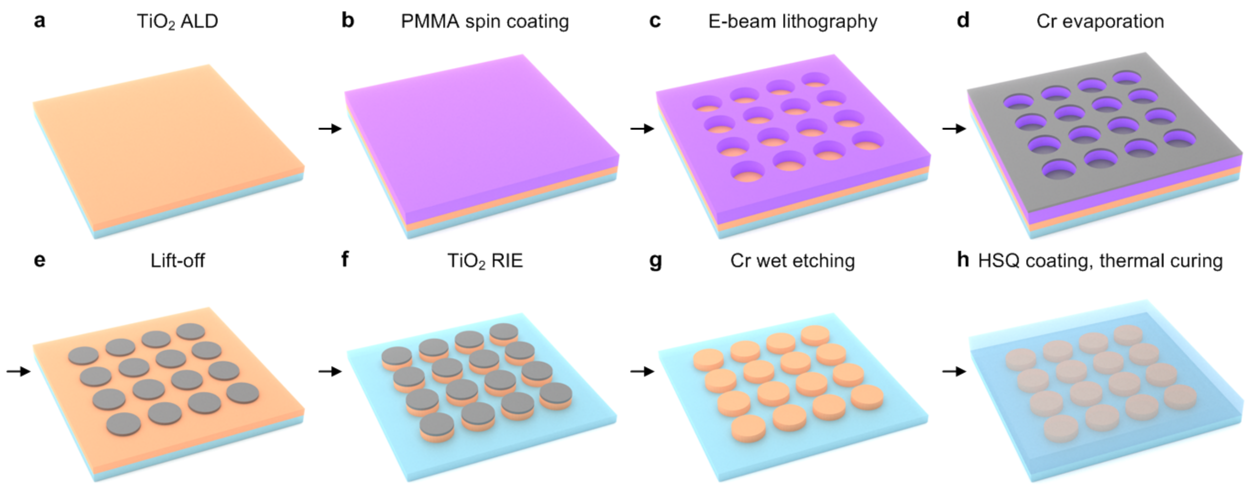

Supplementary Fig. 4 Schematic diagram of the nanofabrication process. (a) A 115 nm TiO_2 layer is deposited on quartz substrate by atomic layer deposition (ALD: precursor TDMATi, at 150 °C), and processed by rapid thermal annealing (RTA: at 475°C for 30 min in O_2) in order to increase its refraction index. (b) The sample is spin-coated with a bilayer of PMMA (MW 495K and 950K, Microchem). (c) The sample is patterned by a single step of e-beam lithography (JEOL JBX-9300FS). After exposure, the Au conductive layer is removed by wet etching, then the sample is developed in MIBK/IPA 3:1 at 4 °C with ultrasonication for 1 min. (d) A 10 nm Cr layer is deposited by e-beam evaporation, (e) leaving Cr discs after lift-off in remover 1165 at 75 °C. (f) The pattern is transferred into the underlying TiO_2 layer by reactive ion etching (RIE: SF_6, 12 sccm, 6 mTorr, 150W). (g) The Cr masks are removed using an aqueous etchant, leaving TiO_2 nanodisc arrays on the quartz substrate. (h) The sample is spin-coated with HSQ and thermally cured (RTA: at 400°C for 15 min in N_2).

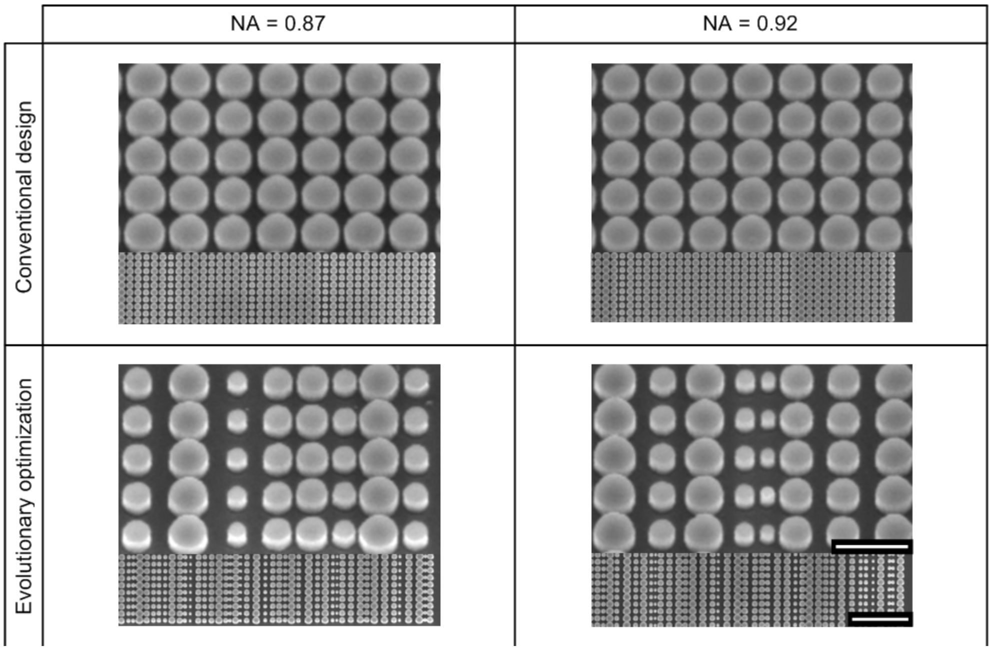

Supplementary Fig. 5 Experimental validation of conventional vs. evolutionary optimization designs. Images of SEM (before HSQ coating) for NA = 0.87, 0.92. Size bar for the SEM is 2 μm, and 500 nm for the zoom-in.

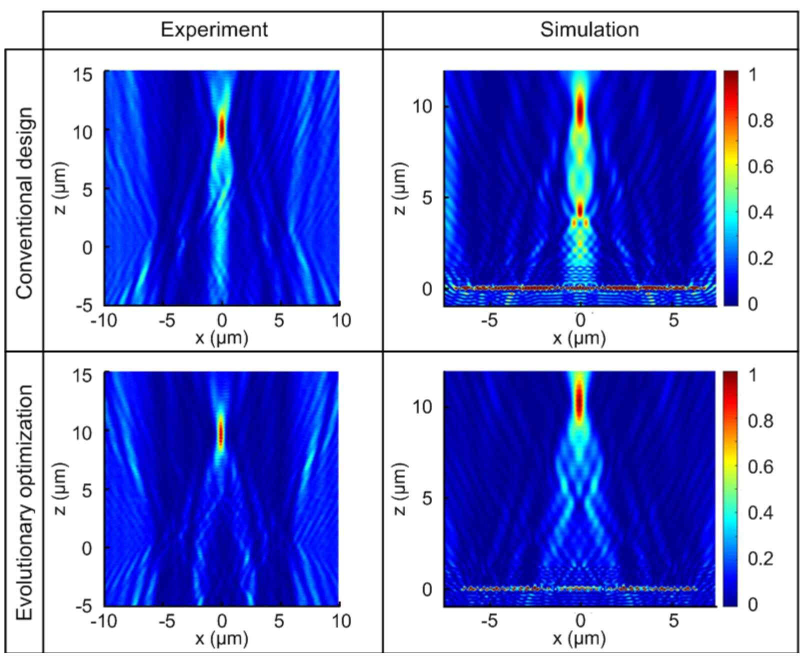

Supplementary Fig. 6 Axial intensity distribution comparison. Experimental and simulation results of conventional vs. evolutionary optimization designs (NA = 0.51).

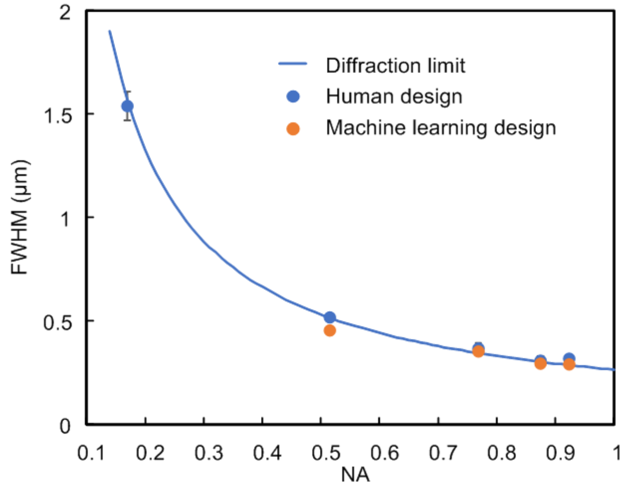

Supplementary Fig. 7 Experimental validation of diffraction-limited focusing. Focal spot size (FWHM) vs. NA. For both conventional and evolutionary optimization designs, the measured focal spots are diffraction-limited for all NAs.

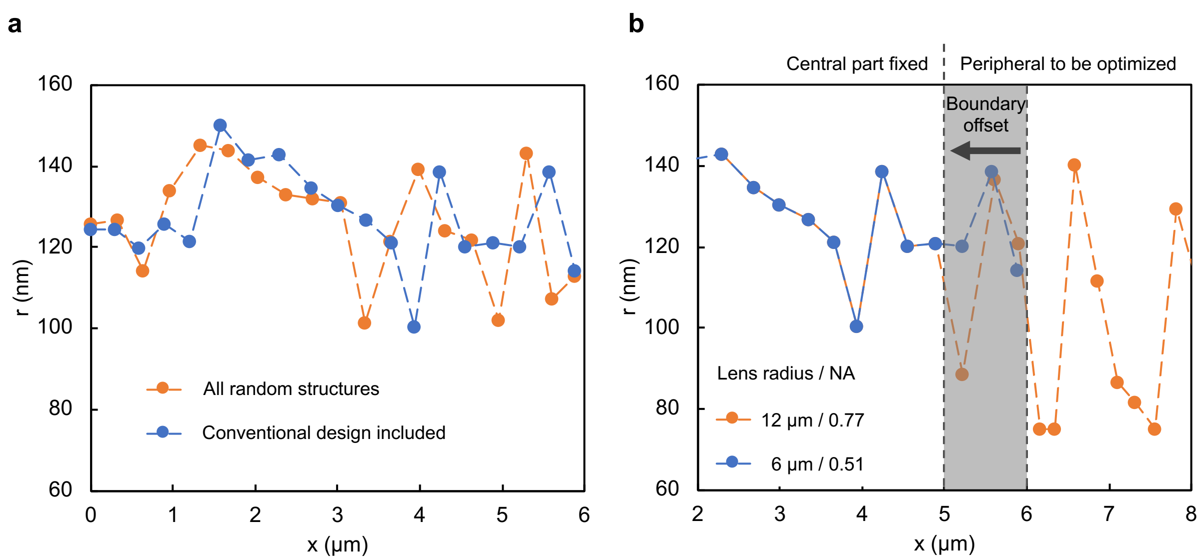

Supplementary Fig. 8 Comparison of EO layouts (nanodisc radius *r* vs. lens radial position *x*). (a) EO starting with all random structures vs. including conventional design in the initial pool (NA 0.51). (b) When designing the lens with a radius of 12 μm (NA 0.77), the central part (5 μm) is fixed the same as the lens with a radius of 6 μm (NA 0.51), and GA is applied for the peripheral 7 μm only. The boundary is offset inward to allow a 1 μm buffer zone, considering nonlocal interactions.